Neuropsychiatric Disease and Treatment

Dovepress

open access to scientific and medical research

Open Access Full Text Article

ORIGINAL RESEARCH

Optimization of an Intranasal Route for the Delivery of Human Neural Stem Cells to Treat a Neonatal Hypoxic-Ischemic Brain Injury Rat Model

Siliang Lu[1,2], Ke Li[1,2], Yinxiang Yang[2], Qian Wang[2], Yu Yu[1,2], Zhaoyan Wang[2], Zuo Luan[1]

[1]The First Clinical Medical College, Guangxi Medical University, Nanning, 530021, Guangxi, People's Republic of China; [2]Laboratory of Pediatrics, The Sixth Medical Center of PLA General Hospital, Beijing, 100048, People's Republic of China

Correspondence: Zhaoyan Wang, Laboratory of Pediatrics, The Sixth Medical Center of PLA General Hospital, Beijing, 100048, People's Republic of China, Tel +86-13581827961, Email wangzhaoyan999@126.com; Zuo Luan, The First Clinical Medical College, Guangxi Medical University, Nanning, Guangxi, 530021, People's Republic of China, Tel +86-18600310270, Fax +86-1066958303, Email luanzuo@aliyun.com

Objective: Stem cell administration via the intranasal route has shown promise as a new therapy for hypoxic-ischemic encephalopathy (HIE). In this study, we aimed to improve the intranasal delivery of stem cells to the brain.

Methods: Human neural stem cells (hNSCs) were identified using immunofluorescence, morphological, and flow cytometry assays before transplantation, and cell migration capacity was examined using the transwell assay. Cerebral hypoxia-ischemia (HI) was induced in 7-day-old rats, followed by the intranasal transplantation of CM-Dil-labeled hNSCs. We examined various experimental conditions, including preconditioning hNSCs with hypoxia, catheter method, multiple low-dose transplantation, head position, cell appropriate concentration, and volume. Rats were sacrificed 1 or 3 days after the final intranasal administration, and parts of the nasal tissue and whole brain sections were analyzed under a fluorescence microscope.

Results: The isolated hNSCs met the characteristics of neural stem cells. Hypoxia (5% O_2, 24 h) enhanced the surface expression of CXC chemokine receptor 4 (CXCR4) (9.21 ± 1.9% ~ 24.76 ± 2.24%, $P < 0.01$) on hNSCs and improved migration (toward stromal cell-derived factor 1 [SDF-1], 0.54 ± 0.11% ~ 8.65 ± 1.76%, $P < 0.001$; toward fetal bovine serum, 8.36 ± 0.81% ~ 21.74 ± 0.85%, $P < 0.0001$). Further improvement increased the number of surviving cell distribution with increased uniformity on the olfactory epithelium and allowed the cells to stay in the nasal cavity for at least 72 h, but they did not survive for longer than 48 h. Optimization of pre-transplantation conditions augmented the success rate of intranasally delivered cells to the brain (0–41.6%). We also tentatively identified that hNSCs crossed the olfactory epithelium into the tissue space below the lamina propria, with cerebrospinal fluid entering the cribriform plate into the subarachnoid space, and then migrated toward injured areas along the brain blood vessels.

Conclusion: This study offers some helpful advice and reference for addressing the problem of repeatability in the intranasal delivery of stem cells.

Keywords: neural stem cell, intranasal, optimization, transplantation, hypoxic-ischemic brain injury

Introduction

Hypoxic-ischemic encephalopathy (HIE) is a neonatal brain injury caused by reduced blood flow and oxygen supply to the neonatal brain and is one of the leading causes of death among infants.[1] As perinatal medicine continues to evolve, the rate of neonatal death has decreased significantly; however, the incidence of nervous system sequelae caused by HIE remains high, such as cerebral palsy, visual disturbance, and hearing loss.[2–4] Unfortunately, HIE treatment remains an unsolved clinical problem.

Received: 30 November 2021
Accepted: 10 February 2022
Published: 23 February 2022

Currently, therapeutic hypothermia is an important treatment option available for HIE, but it is only partially protective.[5] Since treatment strategies are limited for neonates with HIE, developing new, secure, and potent therapies to improve prognosis has great significance. Some preclinical and clinical studies have demonstrated the potential of stem cells for the treatment of HIE.[6–9] Stem cells self-renew throughout life and have the capacity for multipotent differentiation, and are thought to exert their beneficial effects through replacement and paracrine mechanisms when transplanted directly into the injured brain.[10] This implies that stem cell therapies are promising for the treatment of these devastating neonatal disorders.

Stem cells can be delivered into the brain via different routes, and determining the optimal route of stem cell administration is a key problem that needs to be solved in stem cell therapy.[11] In the past decade, the intranasal pathway has been discovered as a new approach for delivering stem cells to the brain.[12] Advantages are that it is non-invasive, and it allows repetitive administration and cell targeting to the site of central nervous system (CNS) lesions. Thus, the intranasal pathway is well suited for unstable and medically fragile infants when compared with other routes for cell transplantation. Many studies have confirmed the therapeutic role of intranasal delivery of stem cells into the brain.[13] However, there are almost no reports on the success rate and stability of intranasally delivered cells into the brain.[14] It is generally accepted that cells transplanted into the brain that migrate to the lesion are crucial for the success of cell therapy in HIE. Nevertheless, clinically, we found that intranasal delivery is not a reliable and stable method. Therefore, it is a very attractive area that deserves further exploration.

In this study, we investigated whether optimization of pre-transplantation conditions augments the success rate of intranasally delivered cells to the brain. Furthermore, we explored the possible entry routes of the CNS for intranasally delivered stem cells.

Materials and Methods

Cell Culture

hNSCs were cultured and passaged as previously described.[15] Briefly, hNSCs were obtained from the surface of the cortex of aborted embryos at 10–13 weeks of gestational age, the protocol was approved by the Ethics Committee of the Navy General Hospital of Chinese PLA (Application No. 2015013). Written informed consent was obtained from each woman who donated aborted fetuses. Primary cells were cultured at a density of 1×10^6 cells/mL in the primary culture medium containing DMEM/F12 (Gibco, Waltham, MA, USA), 1% L-glutamine (Gibco), 1% N_2 supplement (Gibco), 2% B27 supplement (Gibco), basic fibroblast growth factor (bFGF, 20 ng/mL, Peprotech, Rocky Hill, NJ, USA), human recombinant epidermal growth factor (EGF, 20 ng/mL, Peprotech, USA), 5 μg/mL heparin (Sigma, USA), and 2% penicillin/streptomycin (Invitrogen, Carlsbad, CA, USA). Every 3 days, two-thirds of the medium was removed and replaced with a fresh primary culture medium. After 7 days of culture, the expanded cells formed "neurospheres". Next, the neurospheres were trypsinized and passaged in culture flasks containing the primary culture medium, but without B27 supplement.

Hypoxic Preconditioning

To improve the cell migration ability, hNSCs were incubated under hypoxic conditions. To simulate the hypoxic environment, hNSCs were cultured in the presence of 5% O_2 and 8.5% CO_2 and balanced with N_2 in a three-gas incubator (Thermo Scientific Heracell 150i, USA). For in vitro cell migration assay and in vivo experiments, cells were cultured for up to 6 days and then incubated under normoxic or hypoxic conditions for 24 h before testing or harvesting.

Flow Cytometry

To analyze hNSC characterization profiles and CXC chemokine receptor 4 (CXCR4) expression levels, a cognate receptor of stromal cell-derived factor 1 (SDF-1), cells were collected via trypsinization, resuspended in stain buffer (1% fetal bovine serum [FBS] in sterile PBS) at 5×10^5 cells/50 μL and incubated with an Fc blocker for 10 min at 25°C. Cells were then stained with antibodies against Nestin, SOX-2, vimentin, CXCR4 (all from BD Bioscience, CA, USA), or isotype control for 30 min at 4°C. After surface staining, hNSCs were washed once with the abovementioned buffer

and centrifuged at 2000 rpm for 5 min. The obtained cell pellet was resuspended in the same buffer for flow cytometry analysis. Flow cytometry data were processed using FlowJo version 10.4 software (FlowJo, LLC, USA).

Migration Assays

The directed migratory capacities of hNSCs toward SDF-1 or FBS were evaluated using an 8 μm pore Transwell system (Corning, Incorporated, Corning, NY, USA). hNSCs were dissociated into single cells and resuspended in culture media at a density of 2×10^5 cells/mL. Precisely 2×10^4/100 μL of cell solution was plated on top of the filter membrane in a Transwell insert and incubated for 10 min at 37°C and 8.5% CO_2. Next, for the blank control group, 600 μL of hNSC medium was added to the bottom chamber. For the experimental group, 600 μL of hNSC medium containing 10% FBS or 200 ng/mL SDF-1 was used (Peprotech, USA). After 24 h of hypoxia or normoxia treatment at 37°C, the membrane of the Transwell insert was fixed with 4% paraformaldehyde (PFA) in PBS, and cells on top of the membrane were removed with a cotton swab. Cells that migrated to the bottom of the membrane were stained with 4', 6-diamidino-2-phenylindol (DAPI, Solarbio, China). Images were acquired using a fluorescence microscope and the number of cells that had migrated through the membrane toward the chemoattractant and attached to the underside of the membrane was counted using Image J software. All experiments were performed in triplicates.

Cell Labeling

hNSCs were labeled with CM-Dil (Invitrogen) to track and count the cells in the brain. Sterile 1 mM CM-Dil was added, and cells were incubated in the medium for 5 min at 37°C and then for an additional 15 min at 4°C. After labeling, the cells were washed with PBS and resuspended in a fresh medium. Cells were harvested for intranasal delivery after they were cultured for up to 7 days.

Neonatal HI Model

All experiments were approved by the Animal Experiment Ethical Committee of the Sixth Medical Center of the PLA General Hospital Animal Care and Use Committee (Application No. SCXK- 2017-0001). We followed the Laboratory Animal-Guidelines for Ethical Review of Animal Welfare of the People's Republic of China for all protocols regarding animal care and use.

Sprague-Dawley rats on postnatal day 7 were purchased from the Laboratory Animal Center of Peking University. HI was induced as previously described with slight modifications.[16] Rat pups of both sexes were anesthetized via isoflurane (3% induction, 2% maintenance, total duration of surgery: 5 min), and the left common carotid artery of rats was exposed, isolated, and cut using an electrocoagulation knife. After 1 h recovery period with their dams, pups were exposed to hypoxia (8% O_2, 92% N_2) for 90 min at 37°C, and then returned to their mothers after regaining normal color and activity. A total of 32 animals were used for the experiments as follows: 24 for graft success rate analysis (Only male rat pups were used for this part) and 8 for hNSC apoptosis analysis after intranasal delivery.

Intranasal Administration of hNSCs

All pups were divided randomly into two groups as follows: The ordinary transplanted group (n=12) and the optimized transplanted group (n=12). For the ordinary transplanted group, intranasal delivery was performed as previously described with minor modifications,[17] and 3 days after HI induction, the pups were anesthetized with isoflurane (3% induction, 1.5% maintenance) and placed on a heating pad, with the head and neck as parallel to the floor as possible (Figure S1A). Before cell treatment, all pups received intranasal 100 U hyaluronidase (Sigma) dissolved in 8 μL of sterile PBS. Rats received alternate applications (right and left) of 2 μL drops (8 μL total) containing hyaluronidase through the nostrils (twice for each nostril) and then were allowed to fully inhale through the nasal cavity, and the second set of applications was performed 3 min after the First set. Thirty minutes after intranasal pretreatment with hyaluronidase, cell suspensions (1×10^6 in 12 μL of sterile PBS, normoxic) were applied following the same procedure.

A modified intranasal delivery was used for the optimized transplanted group. This protocol was performed based on multiple experiments. Again, a similar method for anesthesia and the same position was used, but a padded pillow made of rolled-up gauze with tapes was placed under the head of the rat (Figure S1B). The key here was that an obtuse angle

was formed between the head and neck. One and 3 days after HI, hyaluronidase (8 μL) or cell suspension (5×10^5 in 20 μL of sterile PBS, hypoxic) was infused into the nasal cavity using a polyethylene catheter (Figure S1C) and the depth of catheter insertion was 5 mm. Injury to the nasal mucosa was avoided, and this position corresponded to the mid-nasal cavity (anatomical distances were obtained via measurements using rat carcasses at the same age and intubation was no longer than 10s). Finally, cell suspensions were applied in alternating 5 μL portions for each nostril. After the operation, we gently shook the body of the rats (similar to head shaking left and right), and then kept them sleeping for 30 min in the supine position. Supine posture was maintained throughout intranasal stem cell delivery. Thus, intranasal delivery was performed using two different approaches, but all animals received an equal number of cells. In addition, subcutaneous injections of cyclosporin A (10 mg/kg) were administered daily to all rats beginning on day three after birth until the animals were sacrificed.

Assessment of Transplanted hNSCs

Exactly 24 and 72 h after the final intranasal administration of hNSCs, rats were sacrificed via CO_2 inhalation, immediately after which they were rapidly decapitated without perfusion, and the brain, nasal mucosa, and trigeminal nerves were removed and postfixed in PFA for 6 h. After fixation, samples were embedded in optimal cutting temperature, frozen in liquid nitrogen, and stored at −80°C. To determine the cellular distribution, migration, and localization of intranasal delivery. Coronal and sagittal equidistant cryosections of sections (16 μm) spanning the whole brain (including parts of nasal tissue) were analyzed (one out of every two sections was picked). Ultimately, a total of 500 slices in the coronal position or 300 slices in the sagittal position were obtained for each animal. Each section was observed under an immunofluorescence microscope after nuclear staining with DAPI, and the number of positive cells was estimated using CM-Dil. The positive cells at a particular location were subjected to double staining with an antibody specific to the human cytoplasm (STEM121). The experimental procedure and flow chart are presented in Figure S2.

Immunofluorescence

Immunofluorescence was used to determine the following factors: (1) Cell differentiation characterization; (2) the positional relationship of positive cells (CM-Dil) in the brain tissue with respect to blood vessels; (3) apoptosis of hNSCs in the nasal cavity after intranasal administration. Briefly, brain sections were thawed and dried at 40°C, followed by fixation in 4% PFA (for STEM121, von Willebrand factor [VWF]) for 10 min at room temperature. The sections were then washed three times with PBS (1×, pH 7.4), 5 min each. Unspecific antibody binding was blocked via incubation with 2% bovine serum albumin (Sigma) for 1 h at room temperature. The cells were then permeabilized using 0.3% Triton X-100 for 5 min, followed by incubation with the following primary antibodies: Mouse monoclonal STEM121 antibody diluted 1:300 (Takara Bio, Japan); mouse monoclonal VWF antibody diluted 1:200 (Santa Cruz Biotech, CA, USA) in PBS overnight at 4°C. Slides were washed with PBS and incubated with goat anti-mouse Alexa Fluor 488 (1:500, Invitrogen) secondary antibody for 1 h at room temperature. Nuclei were detected via DAPI staining.

For cell differentiation characterization, neurospheres were digested into single cells and seeded onto 24-well plates. The culture medium was then replaced with a different cell differentiation medium (all from Gibco, USA). Similarly, after fixation and blocking, the cells were incubated with the following primary antibodies: Rabbit polyclonal Olig-2 antibody diluted 1:500 (Millipore, USA), mouse polyclonal GFAP antibody diluted 1:400 (Abcam, UK), and mouse polyclonal tubulin beta III antibody diluted 1:300 (Abcam, UK) in PBS overnight at 4°C. The secondary antibodies used were as follows: Goat anti-rabbit Alexa Fluor 488 (1:500, Jackson ImmunoResearch Laboratories) and goat anti-mouse Alexa Fluor 488 (1:500, Invitrogen) for 2 h at room temperature. Nuclei were detected via DAPI staining. TUNEL assay was performed using a One-step TUNEL Apoptosis Assay Kit (Beyotime, China). After the anti-fluorescent quenching seal, the results were examined under a fluorescence microscope (IX-70, Olympus, Japan) or a laser confocal microscope (FV3000, Olympus, Japan).

Statistical Analyses

SPSS 23.0, and GraphPad Prism 8.0, were used to analyze the experimental data. The mean ± standard deviation is presented. A two-sample independent-groups *t*-test was used for comparisons between two groups. Statistical significance was defined as a P-value of < 0.05.

Results

Characterization of hNSCs in vitro

The hNSCs were first characterized in vitro according to their growth and differentiation properties. After approximately 7 days in culture, hNSCs proliferated to form neurospheres. This suggested that hNSCs could self-renew and proliferate (Figure 1A). Before intranasal transplantation, we labeled hNSCs with CM-Dil to detect the transplanted cells in the brain. hNSCs were examined using bright field microscopy, and fluorescence microscopy revealed a labeling rate greater than 95% (Figure 1B). The expression of hNSC surface markers was analyzed using flow cytometry. The results demonstrated that our cells expressed a high percentage of typical stem cell markers Nestin, Sox-2, and vimentin at 98.4, 98.5, and 99.9%, respectively (Figure 1C), indicating that high-purity hNSCs were obtained before intranasal administration. For neural differentiation, hNSCs were induced to differentiate for 7–10 days in the differentiation medium, and then cells were immunostained for GFAP, Olig-2, and βIII-tubulin. Results are shown in Figure 1D. These neural stem cells showed multilineage potential to differentiate into astrocytes, oligodendrocytes, and neurons. Taken together, the hNSCs we isolated were of high purity and met the characteristics of neural stem cells.

Hypoxia Induces CXCR4 Expression, Subsequently Promoting hNSC Migration

We tested the effects of hypoxia pretreatment on CXCR4 expression and migration of hNSCs. Flow cytometry revealed that CXCR4 expression on the cell surface was approximately 2.5 times higher in pre-treated hNSCs than that in untreated cells (Figure 2A and B, 24.76±2.24% vs 9.21±1.9%; n=3, $P<0.01$). Next, we tested the effects of hypoxia on hNSC migration. After 24 h of culture in the Transwell culture plates, hypoxia pre-treated hNSCs migrated significantly more than the untreated cells, showing increased migratory capacity toward SDF-1 or FBS (Figure 2C and D, SDF-1, 8.65±1.76% vs 0.54±0.11%, $P<0.001$; FBS, 21.74±0.85% vs 8.36±0.81%; n=3, $P<0.0001$). These results suggested that hypoxia-preconditioned hNSCs had greater migration capacity than normal hNSCs, which was suitable for intranasal transplantation.

Optimized Transplantation Causes a Large Number of Cells to Rest on the Olfactory Mucosa

Two different techniques were used for cell transplantation. The purpose of this was to make more viable hNSCs rest on the olfactory mucosa because we assumed that viable cells might be more likely to cross the cribriform plate and access the brain than a dead cell. Our results showed that transplantation performed using a catheter increased the number of cells in the olfactory epithelium (Table 1). Conversely, natural inhalation caused more cells to stay in the nasal vestibular region, making it very difficult for them to reach the olfactory region (Figures S3 and S4). When natural inhalation was used, almost no hNSCs were found resting in the olfactory region in most cases, 24 or 72 h after intranasal administration (Table 1). This showed that the catheter method was more stable than the natural inhalation method.

Next, hNSC survival in the nasal cavity was examined using the One-step TUNEL Apoptosis Assay Kit. This was performed to choose the interval for multiple transplantations. The results are shown in Figure 3. We found that hNSCs could survive in the nasal cavity for about 24 h (Figure 3A and B), but not longer than 48 h. After 48 h, nearly all cells were stained, showing positive reactions, regardless of hypoxia (Figure 3C and D). These findings confirmed that the grafted cells did not survive for long periods after transplantation, and perhaps the most appropriate interval time of repeated dosing was 24 h for hNSCs.

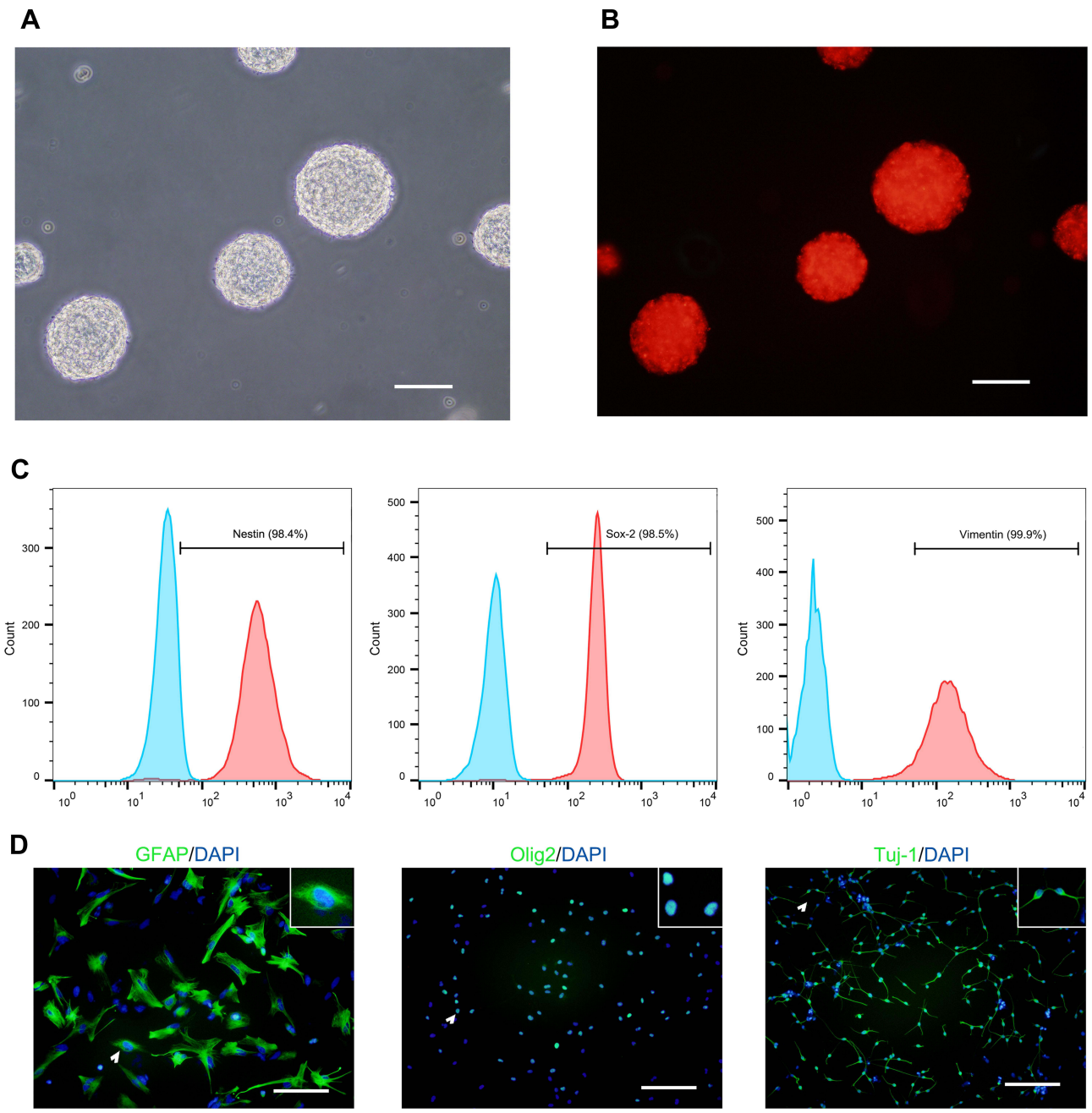

Figure 1 The identification of hNSCs in vitro. (**A**) The morphology of hNSC neurospheres after being cultured for 7 days. (**B**) Fluorescence-labeled cells were observed under a fluorescent microscope. (**C**) Flow cytometry to detect Nestin, Sox-2, and Vimentin of hNSCs. (**D**) hNSCs were cultured in a differentiation condition and immunostained for GFAP, Olig2, and Tuj-1 of hNSCs. Scale bar: 100 μm.

Intranasally Delivered hNSCs Cross the Cribriform and Migrate Along a Blood Vessel Scaffold in the Subarachnoid Space

Sagittal and coronal tissue sections from each rat from the optimization group at different time points were analyzed. To demonstrate that the positive cells at a particular location were hNSCs, we performed double immunofluorescence analysis for STEM121. We initially identified a pathway of intranasally delivered hNSCs entering the brain. The process was as follows: (1) Enter the nasal cavity and rest on the olfactory epithelium; (2) cross the olfactory epithelium into the tissue space below the lamina propria; (3) migrate within the special tissue space; (4) cross the cribriform plate to reach the

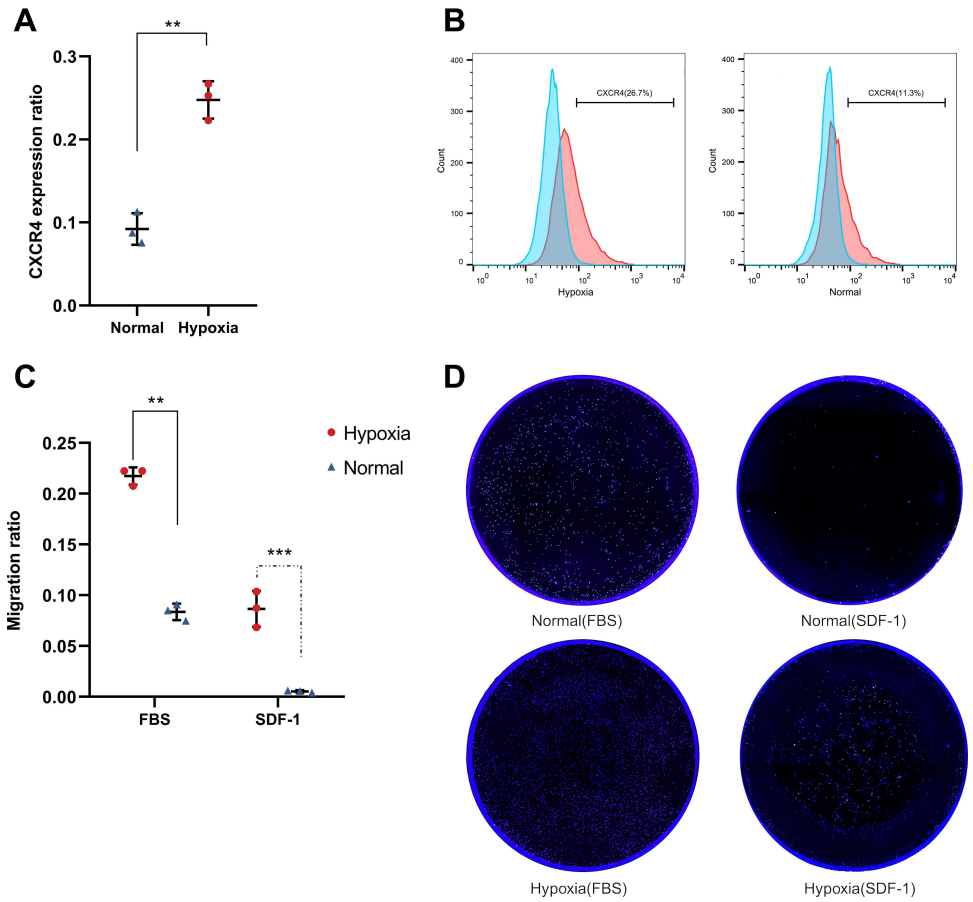

Figure 2 Effect of 5% O_2 on CXCR4 expression and migration in hNSCs. (**A**) Flow cytometry confirms that CXCR4 expression on the cell surface was approximately 2.5 folds higher in hypoxia hNSCs than in growing under normoxic conditions (24.76±2.24% vs 9.21±1.9%; n=3, **P<0.01, 5 vs 21% O_2, Student's *t*-test, error bars show standard deviation). (**B**) Flow cytometry analysis was repeated three times and the figure shows a representative experiment. (**C**) Migration of hNSCs was analyzed using Transwell assay. hNSCs were treated in a hypoxic culture, demonstrating a significant increase in chemotactic migration toward SDF-1- or FBS-containing medium chamber (SDF-1, 8.65±1.76% vs 0.54±0.11%, **P<0.01; FBS, 21.74±0.85% vs 8.36±0.81%; n=3, ***P<0.0001, 5 vs 21% O_2, Student's *t*-test, error bars show standard deviation). (**D**) The Transwell migration experiment was repeated three times and the figure shows a representative experiment.

subarachnoid space; (5) migrate toward injured areas along the brain blood vessels in the subarachnoid space. First, we observed a large number of hNSCs located in the olfactory epithelium. Meanwhile, a small number of cells migrated to the lamina propria close to the turbinate bones (Figure 4A), which was observed in many rats at two time points (24 and 72 h). Interestingly, this phenomenon only occurred in the optimization group; for the ordinary group, hNSCs only rested on the olfactory mucosa. Then, cells migrated in a tissue space beneath the lamina propria and crossed the cribriform plate to reach the subarachnoid space. As shown in Figure 4B, hNSCs were found in spaces between the olfactory nerve and the cribriform plate. This was the subarachnoid space. Finally, these exogenous hNSCs "crawled" along the brain vasculature in the subarachnoid space. Twenty-four hours after the final administration, we observed that hNSCs were mainly located adjacent to a lateral orbitofrontal artery and azygos of the anterior cerebral artery (Figure 4C–E). Furthermore, multi-slice imaging reconstitutions were obtained via confocal microscopy to further demonstrate the relationship between hNSCs and the anterior cerebral artery (Supplementary Video). Over time, hNSCs migrated to the lesioned side of the middle cerebral artery 72 h after the last transplantation (Figure 4F and G). Similarly, hNSCs still had a strong association with blood vessels. Two points are worth noting. First, we did not find hNSCs within the brain parenchyma at any of the time points; second, the hNSCs were found only in the ventral side of the brain and the furthest distance migrated was to the middle cerebral artery.

Table 1 List of Histologic Sections Analysis

Group	Cells Dose	Survival Time (Hour)[a]	Pretreatment	Slice Preparation	No. of Tissue Sections Analyzed	hNSCs on the Olfactory Mucosa[b]	hNSCs into the Brain[c]
Ordinary 1	1.0×10^6	24	/	Coronal	500	Almost no	Fail, =0
Ordinary 2	1.0×10^6	24	/	Coronal	500	Few	Fail, =0
Ordinary 3	1.0×10^6	24	/	Coronal	500	Few	Fail, <10
Ordinary 4	1.0×10^6	24	/	Sagittal	300	Almost no	Fail, =0
Ordinary 5	1.0×10^6	24	/	Sagittal	300	Almost no	Fail, =0
Ordinary 6	1.0×10^6	24	/	Sagittal	300	Much	Fail, =0
Ordinary 7	1.0×10^6	72	/	Coronal	500	Almost no	Fail, =0
Ordinary 8	1.0×10^6	72	/	Coronal	500	Few	Fail, =0
Ordinary 9	1.0×10^6	72	/	Coronal	500	Almost no	Fail, =0
Ordinary 10	1.0×10^6	72	/	Sagittal	300	Almost no	Fail, =0
Ordinary 11	1.0×10^6	72	/	Sagittal	300	Almost no	Fail, =0
Ordinary 12	1.0×10^6	72	/	Sagittal	300	Almost no	Fail, =0
Optimized 1	$0.5\times10^5/\times2$	24	Hypoxia	Coronal	500	Much	Success, >2000
Optimized 2	$0.5\times10^5/\times2$	24	Hypoxia	Coronal	500	Much	Fail, =0
Optimized 3	$0.5\times10^5/\times2$	24	Hypoxia	Coronal	500	Much	Success, >500
Optimized 4	$0.5\times10^5/\times2$	24	Hypoxia	Sagittal	300	Much	Fail, =0
Optimized 5	$0.5\times10^5/\times2$	24	Hypoxia	Sagittal	300	Much	Fail, <100
Optimized 6	$0.5\times10^5/\times2$	24	Hypoxia	Sagittal	300	Much	Fail, <10
Optimized 7	$0.5\times10^5/\times2$	72	Hypoxia	Coronal	500	Much	Success, >2000
Optimized 8	$0.5\times10^5/\times2$	72	Hypoxia	Coronal	500	Few	Success, >500
Optimized 9	$0.5\times10^5/\times2$	72	Hypoxia	Coronal	500	Much	Fail, =0
Optimized 10	$0.5\times10^5/\times2$	72	Hypoxia	Sagittal	300	Much	Success, >3000
Optimized 11	$0.5\times10^5/\times2$	72	Hypoxia	Sagittal	300	Few	Fail, =0
Optimized 12	$0.5\times10^5/\times2$	72	Hypoxia	Sagittal	300	Much	Fail, =0

Notes: [a]Survival time of rats following last intranasal administration of hNSCs. [b]"Almost no": Counts less than 200 or equal to 0; "few": Counts greater than 200 but less than 500; "much": Counts greater than 500; The number of prelabeled-positive cells under a single field of vision (200x magnification). For the sections with the largest numbers of cells. [c]"Fail": There are no or only very few hNSCs into the brain; "Success": There are appreciable amounts of hNSCs into the brain.

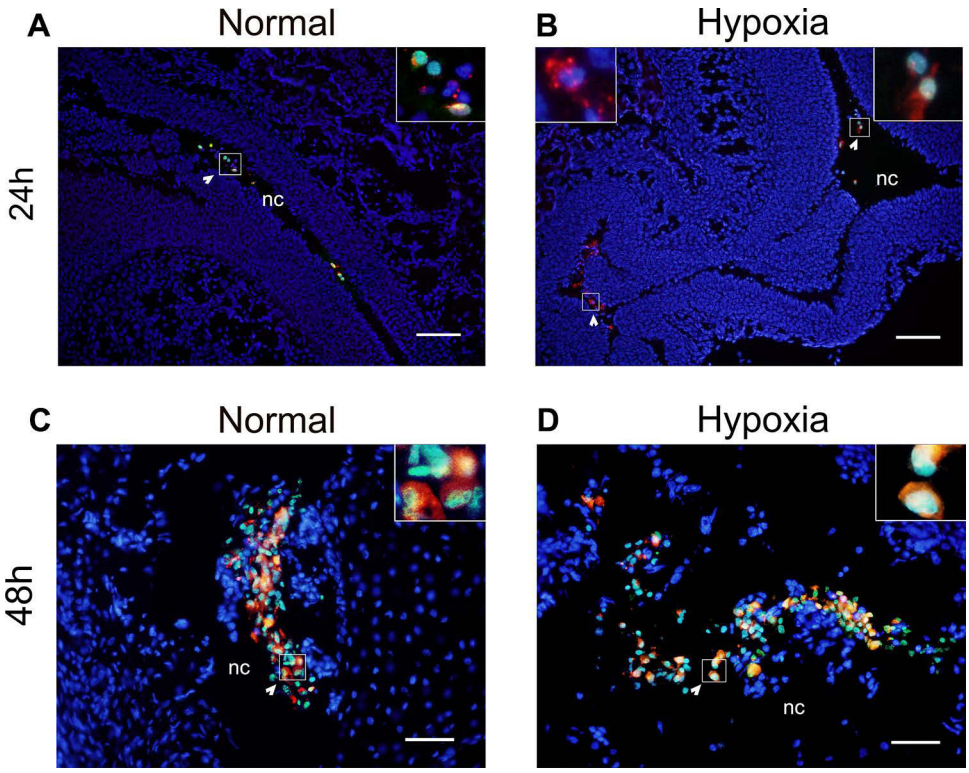

Figure 3 TUNEL analysis after hNSC transplantation under either normoxia or hypoxia. Representative pictures of TUNEL staining, in which red represents CM-Dil, green represents TUNEL, blue represents DAPI staining, each image represents the merge of three captured images. Arrows indicate a series of hNSCs. (**A** and **B**) 24 h after intranasal administration, some hNSC nuclei were detected as green, indicating cells that underwent apoptosis (white arrow). (**C** and **D**) After 48 h, nearly all cells were positive, regardless of hypoxia (white arrow). Scale bars: 200 μm (**A** and **B**), 100 μm (**C** and **D**). n=2.
Abbreviation: nc, nasal cavity.

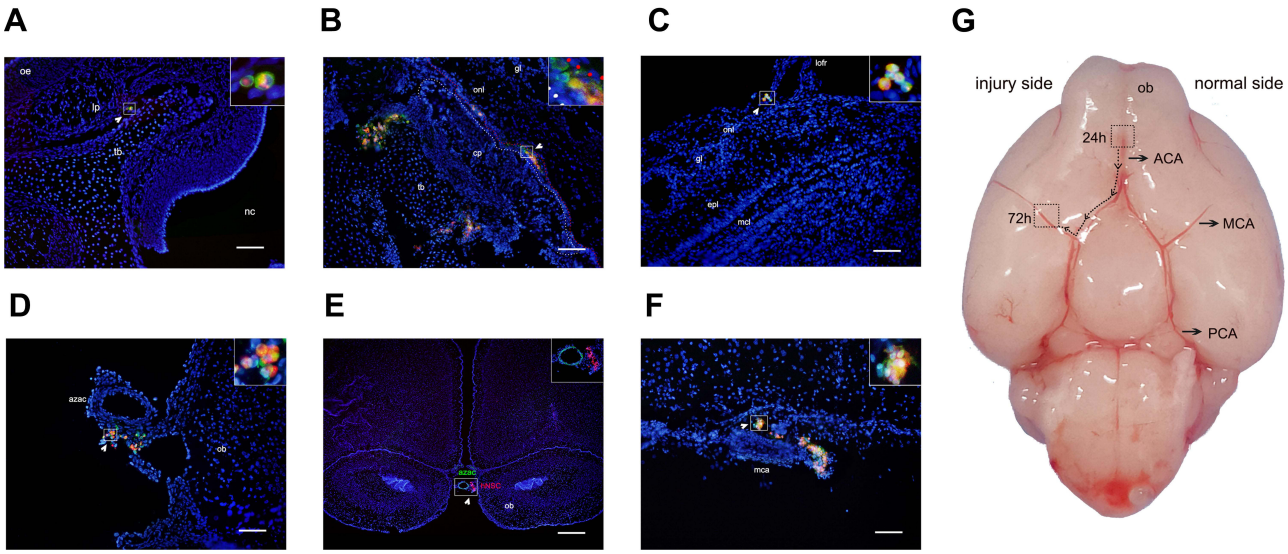

Figure 4 Representative images of the path of cell migration following intranasal administration. Red represents CM-Dil, blue represents DAPI, green represents STEM121 for (**A**–**E**), and vWF staining for (**F**), each image represents the merge of three captured images. Arrows indicate a series of hNSCs. (**A**) Cells are located in tissue space below the lamina propria (lp) (coronal). (**B**) The figure shows the cells cross the cribriform plate (cp) to reach the subarachnoid space, white dashed line indicates the edge of the cp, red dashed line indicates the edge of the olfactory nerve layer (onl) (sagittal). (**C** and **D**) 24 h after intranasal administration, hNSCs were located adjacent to lateral orbitofrontal artery (lofr) and azygos of the anterior cerebral artery (azac) (coronal). (**E**) After 72 h, hNSCs migrated to the lesioned side of the middle cerebral artery (mca) (sagittal). (**F**) Representative images of the relationship between hNSCs and brain vessels (coronal). (**G**) Ventral view of the non-perfused brain surface from a rat on postnatal day 10, the migration route of the hNSCs in the brain was simulated in this figures. Scale bars: 100 μm (**A**–**E**), 500 μm (**F**).
Abbreviations: oe, olfactory epithelium; tb, turbinate bone; nc, nasal cavity; gl, glomerular layer; epl, external plexiform layer; mcl, mitral cell layer; ob, olfactory bulb; ACA, anterior cerebral artery; MCA, middle cerebral artery; PCA, posterior cerebral artery.

Optimized Transplantation Improves the Success Rate of Intranasal Delivery of Cells into the Brain

To rule out development reaction interference and confirm tissue sections, fluorescence double staining for STEM121 was used. Table 1 presents the main results of the study. After a series of optimizations for pre-transplantation conditions, such as hypoxia, use of a microcatheter, and change in the volume of the cell suspension, the number of successful trials increased, but our success rate did not reach 100%. As shown in Table 1, for the optimized group, successful trials were performed in five of the 12 rats (41.6% success). In these rats, we observed relatively appreciable amounts of hNSCs in the brain. However, there were no more than 5×10^3 cells in the brain even in the most successful experiments. In contrast, we were not able to intranasally deliver cells into the brain successfully, even though a large number of hNSCs were located in the nasal cavity on the olfactory mucosa, even when only the ordinary transplantation method was used. Collectively, these data showed that optimized transplantation improved the success rate to some extent.

Discussion

Intranasal application of stem cells in the management of CNS diseases has attracted increasing attention, with over 50 publications demonstrating its potential effectiveness. However, the researchers focused too much on its advantages, while ignoring that intranasal delivery is not a reliable and stable method. This is represented by the number of cells successfully reaching the brain. In the present study, we demonstrated that the success rate of intranasally delivered cells reaching the brain could be improved to some extent by optimizing pre-transplantation conditions. Furthermore, hNSCs could cross the cribriform into the brain via a submucosal tunnel and migrate along a blood vessel scaffold in the subarachnoid space upon intranasal delivery.

Numerous factors affect cells that enter the CNS after intranasal administration. We believe that the main factors contributing to the success of intranasal delivery mainly included the following: Cell function and viability; increased number of cells that adhere to the olfactory epithelium; longer nasal cavity residence time; longer nasal cavity; head position; administration volume. From a cellular perspective, hNSCs that enter the nasal cavity have two possible fates. One such fate is death because a large number of cells are cleared from the nasal cavity and enter the respiratory or digestive tract due to mucus secretion and mucociliary clearance. An alternative fate for the cells is to cross the barrier and undertake long-distance migration to reach the brain lesion. It is proven that high number of surviving cells staying in the nasal cavity is fundamental for the cells to enter the CNS, whereas cell function and viability are key factors. Some studies have demonstrated that NSCs cultured in a low oxygen environment (5%) can increase migration,[18–20] and our results are consistent with these. We adopted the hypoxia pretreatment strategy to improve the hNSC function because it is effective and safe. Interestingly, we could not deliver cells into the brain when untreated cells were used. We believe that this difference may be due to the poor migration of hNSCs. In addition, hypoxia pretreatment strategy can also decrease the apoptosis of NSCs,[20] and indeed, 24 h after intranasal administration, apoptosis was observed in some cells. This proves that hNSCs did not survive long in the nasal cavity after intranasal administration. To address this issue, we chose multiple transplantation times with an interval time of 24 h but it did not change the overall number of cells. One benefit of this is that more cells survive in a fixed period. We note that most of the previous studies used PBS as a single cell suspension, while a few investigators used 2% human serum albumin.[21] This was done to allow increased vitality in a short time before transplantation. However, the time spent from the cell preparation to the end of intranasal delivery was approximately 1 h in practice and PBS could help the cells remain viable throughout this time; therefore, we did not use human serum albumin in the short time before transplantation.

Cells entering the CNS need to cross a substantial barrier, such as the nasal mucosa. In rodents, four types of epithelia can be found in the nasal cavity.[22] These are distributed in diverse locations in the nasal cavity. The epithelium that is most beneficial for cells entering the CNS is probably the olfactory epithelium. In rats, the total area of the olfactory epithelium covers 50% of the nasal cavity surface,[22–24] whereas the olfactory nerve terminates at the apical surface of the olfactory epithelium and is in direct contact with the external environment and the olfactory bulbs. The olfactory bulb is the first location after intranasal (IN) cells.[12,25–27] Another direct pathway from the nose to the brain is the trigeminal nerve, but it is relatively long compared to the olfactory nerve. The olfactory nerve is not the only neuron invading the

nasal mucosa, the ophthalmic branches of the trigeminal nerve innervate the olfactory epithelium.[28] Thus, if cells are to enter the CNS from the nasal mucosa through the nerve pathway, the olfactory epithelium is a good choice. The nasal mucosa is covered with mucus. Foreign substances, such as particles and bacteria can be entrapped by the mucus, and these substances are cleared by the consistent whip-like action of cilia.[29,30] Therefore, mucociliary clearance affects the residence time of cells in the nasal cavity. Spencer et al sought to mechanically delay the rapid clearance of hNSCs by the ciliated epithelium from the nasal cavity using fibrin glue,[31] and although fibrin glue had some effect, it was less pronounced. This proves that mucociliary clearance has a strong scavenging capability; however, olfactory cilia are described as immotile due to the lack of dynein, which is essential for motility.[32] Thus, cells are markedly more likely to adhere to the olfactory epithelium. Similar findings were observed in the present study. We adopted a combination of multiple transplantations using the polyethylene catheter strategy and gently shaking the body of the rats after intranasal administration. By doing this, more surviving cells were distributed uniformly on the olfactory epithelium, which stayed in the nasal cavity for a relatively long period. Meanwhile, cell deposition in other epithelium was largely avoided.

We also considered the influence of the head position and volume of the cell suspension. We have been actively looking for a suitable solution volume for intranasal delivery, where a small volume will likely result in less surface area to cover and a large volume will result in more cells in the respiratory or digestive tract, which could even lead to respiratory distress. Finally, we chose to use approximately 30% of the nasal cavity volume as an administration volume, because this volume ensures that the entire nasal cavity, including the olfactory region, is well exposed.[33] The nasal cavity volume of rats was estimated using a previously published formula,[34] and all similar experiments refer to this formula. The choice of the appropriate concentration of the right cell is extremely important as well because high cell concentration is unfavorable for cell migration (at least in our study). We propose that it should be below $10^5/\mu L$. In addition to the above factors, the head position is equally important for intranasal delivery. For a human, the best head position for intranasal delivery of cells or drugs is via contact with the olfactory epithelium, which is called the "Praying to mecca position".[35,36] Only 8% of the nasal cavity surface area is the olfactory region in humans, principally centered near the cribriform plate. Critically, the cribriform plate is parallel to the ground level.[37] However, due to the different anatomy in rats, the horizontal position was the best, but some improvements were needed. The olfactory epithelium covers a larger percentage of the nasal cavity in rodents (approximately 50%). In the normal posture, the cribriform plate demonstrated an acute angle with the ground in rats. In other words, the cribriform plate was at a slant. One study showed the deposition and distribution within the nasal cavity in a supine position of the head at a 40° angle to the bed.[38] During 1 h, increasing amounts of the swallowed drug were observed in the oropharynx. Therefore, for intranasal delivery of cells, the head should be as parallel to the floor as possible with a padded pillow under the head of the rat. Furthermore, an obtuse angle must be formed between the head and neck, to avoid swallowed cells.

Currently, the mechanism of intranasal delivery of cells into the CNS is not very clear, and scholars have put forward a series of hypotheses, such as the perineural, perivascular, and cerebrospinal fluid (CSF) pathways; however, these pathways seem to be interconnected. Initially, we found that hNSCs were localized in the olfactory epithelium and the tissue space below the lamina propria, which is consistent with the results of Galeano et al.[39] This illustrates that hNSCs can cross the olfactory epithelium in a unique way. The olfactory epithelium consists of supporting cells and olfactory sensory neurons with tight junction proteins between them and it restricts the paracellular permeability of the epithelium.[40,41] Some substances, such as viruses and small or large molecules, can cross the "barriers" via the transcellular or paracellular pathway. However, this seems unlikely for hNSCs, as the size between hNSCs and tight junctions differ substantially.[42] Therefore, hNSCs could pass through the olfactory epithelium through existing gaps in the mucosa created by the natural shedding of epithelial cells.[43] However, these "entrances" to the brain appears to be randomly distributed on the mucosa. Perhaps this explains why intranasal delivery of cells is not a reliable and stable method, and this is another reason why we adopted multiple transplantation strategies. Multiple investigations have suggested that the subarachnoid space and nasal mucosa potentially communicate.[44,45] Kida et al investigated the CSF drainage pathways from the rat brain by injecting Indian ink into the cisterna magna and found that Indian ink passed from the subarachnoid space through the cribriform plate, often but not always, alongside nasal nerves, passing into the olfactory submucosa.[46] hNSCs were found at the same position in our study, indicating that the tissue space underlying the nasal mucosa contains the CSF and allows cells to migrate. We then observed hNSCs crossing the cribriform plate to reach the

subarachnoid space, which was observed at both time points (24 and 72 h). We considered this reverse migration dynamic to be powered by the bidirectional flow of the CSF.[41,47] In other words, hNSCs accessing the subarachnoid space following intranasal administration could potentially be distributed along the direction of CSF flow to other, more distant sites. This could explain why cells are distributed to the hippocampus, cerebellum, and around the injury area in a very short period.[12,27] An alternative explanation is that cells can move through the trigeminal pathway to reach the CNS, but here, we have not observed similar phenomena. hNSCs were found predominantly surrounding the vasculature at two time points in our study, indicating that there are at least two ways for hNSCs to be distributed in the CNS after entering the subarachnoid space, one relatively fast and the other relatively slow. Our results showed the latter, where the farthest distance of cell migration was only the middle cerebral artery. We speculate that the cell migration route follows the subarachnoid space from 24 to 72 h. hNSCs migrated along a blood vessel scaffold from rostral to caudal side. This also illustrates why hNSCs were found only on the ventral side of the brain. Therefore, our study indicated that the intranasal administration of exogenous stem cells had the same mode of cell migration as the endogenous stem cells after ischemic brain injury.[48] Unlike many other studies, hNSC migration to the region of injury was not observed at arbitrary time points.[49–52] Moreover, the number of hNSCs entering the brain was not high. This was probably due to the different migration capacities of the different cell types. After 24 h of HIE, a variety of chemokines, such as SDF-1, are constitutively secreted by astrocytes and vascular endothelial cells in the region of injury and promote the migration of neuroblasts that express the relevant receptor toward injured regions.[53–57] Approximately 30% of migrating neuroblasts in the injured brain travel along blood vessels.[56,58] This highlights the importance of the cerebral vasculature for the repair of brain injury and chemoattractants in the control of cell migration to sites of brain injury.

Nevertheless, the shortcomings of the current study need to be addressed. First, we only used a newborn rat model of HIE and did not use large animals and other CNS disease models to validate our hypothesis. We need to consider the specificity of the nasal structure in rodents, as well as the different pathogenesis of CNS diseases. Second, additional types of stem cells are required to verify this optimization strategy, because functions and properties vary between different types of stem cells. We believe that these limitations do not affect our main conclusions. However, further efforts are warranted to prove these ideas.

Conclusion

In conclusion, we demonstrated that optimization of pre-transplantation conditions augments the efficacy of intranasally delivered cells to the brain to a certain extent, and tentatively identified one pathway of intranasally delivered hNSCs entering the brain. However, studies on intranasal delivery of stem cells as a CNS disease therapy remain at an early stage, and much remains to be done. In the future, more studies should be carried out investigating the mechanisms of transnasal transport routes of stem cells, the reproducibility and efficiency of delivery, and safety.

Acknowledgments

We would like to thank Editage for English language editing.

Funding

This research was supported by the National Key R&D Program of China (NO.2017YFA0104200).

Disclosure

The authors report no conflicts of interest in this work.

References

1. Ferriero DM. Neonatal brain injury. *N Engl J Med*. 2004;351(19):1985–1995. doi:10.1056/NEJMra041996
2. Glinianaia SV, Best KE, Lingam R, Rankin J. Predicting the prevalence of cerebral palsy by severity level in children aged 3 to 15 years across England and Wales by 2020. *Dev Med Child Neurol*. 2017;59(8):864–870. doi:10.1111/dmcn.13475
3. Goldstein M. The treatment of cerebral palsy: what we know, what we don't know. *J Pediatr*. 2004;145(2–supp–S):S42–S46. doi:10.1016/j.jpeds.2004.05.022
4. Gulczyńska E, Gadzinowski J. Therapeutic hypothermia for neonatal hypoxic-ischemic encephalopathy. *Ginekol Pol*. 2012;45(3):214–218.

5. Cho KH, Davidson JO, Dean JM, Bennet L, Gunn AJ. Cooling and immunomodulation for treating hypoxic-ischemic brain injury. *Pediatr Int*. 2020;62(7):770–778. doi:10.1111/ped.14215
6. Ahn SY, Chang YS, Sung DK, Sung SI, Park WS. Hypothermia broadens the therapeutic time window of mesenchymal stem cell transplantation for severe neonatal hypoxic ischemic encephalopathy. *Sci Rep*. 2018;8(1):7665. doi:10.1038/s41598-018-25902-x
7. Douglas-Escobar M, Weiss MD. Hypoxic-ischemic encephalopathy: a review for the clinician. *JAMA Pediatr*. 2015;169(4):397–403. doi:10.1001/jamaPediatrics.2014.3269
8. Li F, Zhang K, Liu H, Yang T, Wang YS, Wang Y-S. The neuroprotective effect of mesenchymal stem cells is mediated through inhibition of apoptosis in hypoxic ischemic injury. *World J Clin Pediatr*. 2019;16(2):193–200. doi:10.1007/s12519-019-00310-x
9. Tsuji M, Sawada M, Watabe S, Sano H, Shintaku H. Autologous cord blood cell therapy for neonatal hypoxic-ischaemic encephalopathy: a pilot study for feasibility and safety. *Sci Rep*. 2020;10(1):4603. doi:10.1038/s41598-020-61311-9
10. Li T, Xia M, Gao Y, Chen Y, Xu Y. Human umbilical cord mesenchymal stem cells: an overview of their potential in cell-based therapy. *Expert Opin Biol Ther*. 2015;15(9):1–14. doi:10.1517/14712598.2015.1051528
11. Zhang S, Lachance BB, Moiz B, Jia X. Optimizing stem cell therapy after ischemic brain injury. *J Stroke*. 2020;22(3):286–305. doi:10.5853/jos.2019.03048
12. Danielyana L, Scha¨fer R, Ameln-Mayerhofer A, et al. Intranasal delivery of cells to the brain. *Eur J Cell Biol*. 2009;88(6):315–324. doi:10.1016/j.ejcb.2009.02.001
13. Zhang YT, He KJ, Zhang JB, Ma QH, Liu CF, Liu C-F. Advances in intranasal application of stem cells in the treatment of central nervous system diseases. *Stem Cell Res Ther*. 2021;12(1):210. doi:10.1186/s13287-021-02274-0
14. Lee ES, Im HJ, Kim HS, et al. In vivo brain delivery of v-myc overproduced human neural stem cells via the intranasal pathway: tumor characteristics in the lung of a nude mouse. *Mol Imaging*. 2015;14:1–10. doi:10.2310/7290.2014.00042
15. Du Q, Yang Y, Wang Z, et al. Isolation and culture of human oligodendrocyte precursor cells from neurospheres. *Brain Res Bull*. 2015;118:17–24. doi:10.1016/j.brainresbull.2015.08.008
16. Rice JE, Vannucci RC, Brierley JB. The influence of immaturity on hypoxic-ischemic brain damage in the rat. *Ann Neurol*. 1981;9(2):131–141. doi:10.1002/ana.410090206
17. Hanson LR, Fine JM, Svitak AL, Faltesek KA. Intranasal administration of CNS therapeutics to awake mice. *J Vis Exp*. 2013;8(74):4440. doi:10.3791/4440
18. Dey M, Yu D, Kanojia D, et al. Intranasal oncolytic virotherapy with CXCR4-enhanced stem cells extends survival in mouse model of glioma. *Stem Cell Rep*. 2016;7(3):471–482. doi:10.1016/j.stemcr.2016.07.024
19. Wakai T, Narasimhan P, Sakata H, Wang E, Chan PH. Hypoxic preconditioning enhances neural stem cell transplantation therapy after intracerebral hemorrhage in mice. *J Cereb Blood Flow Metab*. 2015;36(12):2134–2145. doi:10.1177/0271678X15613798
20. Wang Y, Yang L, Wang Y. Enhanced differentiation of neural stem cells to neurons and promotion of neurite outgrowth by oxygen-glucose deprivation. *Int J Dev Neurosci*. 2015;43:50–57. doi:10.1016/j.ijdevneu.2015.04.009
21. Gutova M, Cheng JP, Adhikarla V, et al. Intranasally administered L-Myc-immortalized human neural stem cells migrate to primary and distal sites of damage after cortical impact and enhance spatial learning. *Stem Cells Int*. 2021;2021:5549381. doi:10.1155/2021/5549381
22. Uraih LC, Maronpot RR. Normal histology of the nasal cavity and application of special techniques. *Environ Health Perspect*. 1990;85:187–208. doi:10.1289/ehp.85-1568325
23. Gross EA, Swenberg JA, Fields S, Popp JA. Comparative morphometry of the nasal cavity in rats and mice. *J Anat*. 1982;135(Pt 1):83–88.
24. Harkema JR. Comparative pathology of the nasal mucosa in laboratory animals exposed to inhaled irritants. *Environ Health Perspect*. 1990;85:231–238. doi:10.1289/ehp.85-1568334
25. Fransson M, Piras E, Wang H, et al. Intranasal delivery of central nervous system-retargeted human mesenchymal stromal cells prolongs treatment efficacy of experimental autoimmune encephalomyelitis. *Immunology*. 2014;142(3):431–441. doi:10.1111/imm.12275
26. Wei ZZ, Wei ZZ, Gu X, et al. Intranasal delivery of hypoxia-preconditioned bone marrow-derived mesenchymal stem cells enhanced regenerative effects after intracerebral hemorrhagic stroke in mice. *Exp Neurol*. 2015;272:78–87. doi:10.1016/j.expneurol.2015.03.011
27. Wei N, Yu SP, Gu X, et al. Delayed intranasal delivery of hypoxic-preconditioned bone marrow mesenchymal stem cells enhanced cell homing and therapeutic benefits after ischemic stroke in mice. *Cell Transplant*. 2013;22(6):977–991. doi:10.3727/096368912X657251
28. Silver WL, Finger TE. The anatomical and electrophysiological basis of peripheral nasal trigeminal chemoreception. *Ann NY Acad Sci*. 2010;1170:202–205. doi:10.1111/j.1749-6632.2009.03894.x
29. Soane RJ, Frier M, Perkins AC, Jones NS, Davis SS, Illum L. Evaluation of the clearance characteristics of bioadhesive systems in humans. *Int J Pharm*. 1999;178(1):55–65. doi:10.1016/s0378-5173(98)00367-6
30. Schuhl JF. Nasal mucociliary clearance in perennial rhinitis. *J Investig Allergol Clin Immunol*. 1995;5(6):333–336.
31. Spencer D, Yu D, Morshed RA, et al. Pharmacologic modulation of nasal epithelium augments neural stem cell targeting of glioblastoma. *Theranostics*. 2019;9(7):2071–2083. doi:10.7150/thno.29581
32. Sankaran S, Khot LR, Panigrahi S. Biology and applications of olfactory sensing system: a review. *Sens Actuators B Chem*. 2012;171–172:1–17. doi:10.7150/thno.29581
33. Kuboyama Y, Mori K, Suzuki K, Ishii A, Shuto K. Changes in nasal cavity volume and target area of exposure to nasal drops with age in rats. *Exp Anim*. 1996;45(1):15–22. doi:10.1538/expanim.45.15
34. Ménache MG, Hanna LM, Gross EA, et al. Upper respiratory tract surface areas and volumes of laboratory animals and humans: considerations for dosimetry models. *J Toxicol Environ Health*. 1997;50(5):475–506. doi:10.1080/00984109708984003
35. Merkus P, Ebbens FA, Muller B, Fokkens WJ. Influence of anatomy and head position on intranasal drug deposition. *Eur Arch Otorhinolaryngol Head Neck*. 2006;263(9):827–832. doi:10.1007/s00405-006-0071-5
36. Raghavan U, Logan BM. New method for the effective instillation of nasal drops. *J Laryngol Otol*. 2000;114(6):456–459. doi:10.1258/0022215001905832
37. Lochhead JJ, Thorne RG. Intranasal delivery of biologics to the central nervous system. *Adv Drug Deliv Rev*. 2012;64(7):614–628. doi:10.1016/j.addr.2011.11.002
38. Ponto L, Walsh S, Huang J, et al. Pharmacoimaging of blood-brain barrier permeable (FDG) and impermeable (FLT) substrates after intranasal (IN) administration. *AAPS J*. 2018;20(1):15. doi:10.1208/s12248-017-0157-6

39. Galeano C, Qiu Z, Mishra A, et al. The route by which intranasally delivered stem cells enter the central nervous system. *Cell Transplant*. 2018;27:501–514. doi:10.1177/0963689718754561
40. Steinke A, Meier-Stiegen S, Drenckhahn D, Asan E. Molecular composition of tight and adherens junctions in the rat olfactory epithelium and fila. *Histochem Cell Biol*. 2008;130(2):339–361. doi:10.1007/s00418-008-0441-8
41. Wolburg H, Wolburg-Buchholz K, Sam H, Horvát S, Deli MA, Mack AF. Epithelial and endothelial barriers in the olfactory region of the nasal cavity of the rat. *Histochem Cell Biol*. 2008;130(1):127–140. doi:10.1007/s00418-008-0410-2
42. Costantino HR, Illum L, Brandt G, Johnson PH, Quay SC. Intranasal delivery: physicochemical and therapeutic aspects. *Int J Pharm*. 2007;337(1–2):1–24. doi:10.1016/j.ijpharm.2007.03.025
43. Kincaid AE, Ayers JI, Bartz JC, Caughey BW. Specificity, size, and frequency of spaces that characterize the mechanism of bulk transepithelial transport of prions in the nasal cavities of hamsters and mice. *J Virol*. 2016;90(18):8293–8301. doi:10.1128/JVI.01103-16
44. Johnston M, Zakharov A, Papaiconomou C, Salmasi G, Armstrong D. Evidence of connections between cerebrospinal fluid and nasal lymphatic vessels in humans, non-human primates and other mammalian species. *Cerebrospinal Fluid Res*. 2004;1(1):2. doi:10.1186/1743-8454-1-2
45. Yoffey JM, Drinker CK. The lymphatic pathway from the nose and pharynx, the absorption of dyes. *J Exp Med*. 1938;68(6):629–640. doi:10.1084/jem.68.4.629
46. Kida S, Pantazis A, Weller RO. CSF drains directly from the subarachnoid space into nasal lymphatics in the rat. anatomy, histology and immunological significance. *Neuropathol Appl Neurobiol*. 1994;19(6):480–488.
47. Faber WM. The nasal mucosa and the subarachnoid space. *Dev Dyn*. 1937;62(1):121–148.
48. Jinno H. Regeneration using endogenous neural stem cells following neonatal brain injury. *Pediatr Int*. 2020;63:13–21. doi:10.1111/ped.14368
49. Donega V, Nijboer CH, Braccioli L, et al. Intranasal administration of human msc for ischemic brain injury in the mouse: in vitro and in vivo neuroregenerative functions. *PLoS One*. 2014;9:e112339. doi:10.1371/journal.pone.0112339
50. Donega V, Nijboer CH, Tilborg GV, Dijkhuizen RM, Kavelaars A, Heijnen CJ. Intranasally administered mesenchymal stem cells promote a regenerative niche for repair of neonatal ischemic brain injury. *Exp Neurol*. 2014;261:53–64. doi:10.1016/j.expneurol.2014.06.009
51. Inoue T, Sugiyama M, Hattori H, Wakita H, Wakabayashi T, Ueda M. Stem cells from human exfoliated deciduous tooth-derived conditioned medium enhance recovery of focal cerebral ischemia in rats. *Tissue Eng Part A*. 2013;19(1–2):24–29. doi:10.1089/ten.TEA.2011.0385
52. Velthoven CV, Kavelaars A, Bel FV, Heijnen CJ. Nasal administration of stem cells: a promising novel route to treat neonatal ischemic brain damage. *Pediatr Res*. 2010;419–422. doi:10.1203/PDR.0b013e3181f1c289
53. Jiang L, Newman M, Saporta S, et al. MIP-1alpha and MCP-1 induce migration of human umbilical cord blood cells in models of stroke. *Curr Neurovasc Res*. 2008;5(2):118–124. doi:10.2174/156720208784310259
54. Qin Y, Liu L, Jie L, Yan W, Hu S. SDF-1α/CXCR4 axis mediates the migration of mesenchymal stem cells to the hypoxic-ischemic brain lesion in a rat model. *Cell J*. 2015;16(4):440–447. doi:10.22074/cellj.2015.504
55. Rosenkranz K, Kumbruch S, Lebermann K, et al. The chemokine SDF-1/CXCL12 contributes to the 'homing' of umbilical cord blood cells to a hypoxic-ischemic lesion in the rat brain. *J Neurosci Res*. 2010;88(6):1223–1233. doi:10.1002/jnr.22292
56. Thored P, Wood J, Arvidsson A, Cammenga J, Kokaia Z, Lindvall O. Long-term neuroblast migration along blood vessels in an area with transient angiogenesis and increased vascularization after stroke. *Stroke*. 2007;38(11):3032–3039. doi:10.1161/STROKEAHA.107.488445
57. Gong Y, Fan Y, Hoover-Plow J. Plasminogen regulates stromal cell-derived factor-1/cxcr4-mediated hematopoietic stem cell mobilization by activation of matrix metalloproteinase-9. *Arterioscler Thromb Vasc Biol*. 2011;31(9):2335–2343. doi:10.1161/ATVBAHA.111.229583
58. Kojima T, Hirota Y, Ema M, et al. Subventricular zone-derived neural progenitor cells migrate along a blood vessel scaffold toward the post-stroke striatum. *Stem Cells*. 2010;28:545–554. doi:10.1002/stem.306